water

MDPI

Article

Supplementary Materials

Modeling Cyanobacteria Vertical Migration

Corina Overman * and Scott Wells

Department of Civil and Environmental Engineering, Portland State University, P.O. Box 751, Portland, OR 97207-0751, USA; wellss@pdx.edu
* Correspondence: corinaoverman@gmail.com

1. Model Equations

Table S1. Predefined velocity models used in continuum framework.

Model	Equations	
Time-varying velocity	$v_{p_i}^n > 0,\quad c_i^{n+1} = \frac{D_z\Delta t}{\Delta z^2}(c_{i+1}^n - 2c_i^n + c_{i-1}^n) - \frac{\Delta t}{\Delta z}(v_{p_i}^n c_i^n - v_{p_{i-1}}^n c_{i-1}^n) + (\mu_{net}\Delta t + 1)c_i^n$	19
	$v_p^n < 0,\quad c_i^{n+1} = \frac{D_z\Delta t}{\Delta z^2}(c_{i+1}^n - 2c_i^n + c_{i-1}^n) - \frac{\Delta t}{\Delta z}(v_{p_{i+1}}^n c_{i+1}^n - v_{p_i}^n c_i^n) + (\mu_{net}\Delta t + 1)c_i^n$	20
	$v_p(t) = A\frac{2\pi}{86{,}400\ s}cos\left(\frac{2\pi}{86{,}400\ s}t + \phi\right)$	22
Belov & Giles [4]	$v_{p_i}^n > 0,\quad c_i^{n+1} = \frac{D_z\Delta t}{\Delta z^2}(c_{i+1}^n - 2c_i^n + c_{i-1}^n) - \frac{\Delta t}{\Delta z}(v_{p_i}^n c_i^n - v_{p_{i-1}}^n c_{i-1}^n) + (\mu_{net}\Delta t + 1)c_i^n$	19
	$v_p^n < 0,\quad c_i^{n+1} = \frac{D_z\Delta t}{\Delta z^2}(c_{i+1}^n - 2c_i^n + c_{i-1}^n) - \frac{\Delta t}{\Delta z}(v_{p_{i+1}}^n c_{i+1}^n - v_{p_i}^n c_i^n) + (\mu_{net}\Delta t + 1)c_i^n$	20
	$v_p(t,z) = \begin{cases} A\frac{2\pi}{86{,}400\ s}cos\left(\frac{2\pi}{86{,}400\ s}t + \phi\right)e^{-\alpha(H-z)}, & I_0 > 0 \\ A\frac{2\pi}{86{,}400\ s}cos\left(\frac{2\pi}{86{,}400\ s}t + \phi\right), & I_0 \le 0 \end{cases}$	23

Table S2. Predefined velocity models used in particle-tracking framework.

Model	Equations	
Time-varying velocity	$z_{p_i}^{n+1} = z_{p_i}^n + v_{p_i}^n\Delta t + R\sqrt{6D_{z_i}^n\Delta t}$	21
	$v_p(t) = A\frac{2\pi}{86{,}400\ s}cos\left(\frac{2\pi}{86{,}400\ s}t + \phi\right)$	22
Belov & Giles [4]	$z_{p_i}^{n+1} = z_{p_i}^n + v_{p_i}^n\Delta t + R\sqrt{6D_{z_i}^n\Delta t}$	21
	$v_p(t,z) = \begin{cases} A\frac{2\pi}{86{,}400\ s}cos\left(\frac{2\pi}{86{,}400\ s}t + \phi\right)e^{-\alpha(H-z)}, & I_0 > 0 \\ A\frac{2\pi}{86{,}400\ s}cos\left(\frac{2\pi}{86{,}400\ s}t + \phi\right), & I_0 \le 0 \end{cases}$	23

Table S3. Converted parameter values from Visser et al. [13] using conversion factor of 2 $\mu mol\ photon\ s^{-1}/Watt$ [48].

Parameter	I_c, $W\ m^{-2}$	c_1, $s^2\ m^{-3}$	c_2, $kg\ m^{-3}s^{-2}$	f_1, s^{-1}	f_2, $kg\ m^{-3}\ s^{-1}$
Converted Value	5.45	$5.333x10^{-5}$	$-2.75x10^{-4}$	$-1.587x10^{-}$	0.0164

Table S4. Dynamic velocity models used in continuum framework.

Model	Equations	
Growth kinetics	$v_p = \frac{2gr^2(\rho_c-\rho')A}{9\phi n}$	2
	$\mu_{net} = \mu_{g,max}F(I) - \mu_r - \mu_e - \mu_m$	25
	$\rho_{c_i}^{n+1} = \rho_{c_i}^n \mu_{net_i}^n \Delta t + \rho_{c_i}^n$	28
	$c_i^{n+1} = \frac{D_z\Delta t}{\Delta z^2}(c_{i+1}^n - 2c_i^n + c_{i-1}^n) - \frac{\Delta t}{\Delta z}\left(\lvert v_{p_i}^n c_i^n\rvert - v_{p_B}^n c_{i+1}^n - v_{p_T}^n c_{i-1}^n\right) + (\mu_{net}\Delta t + 1)c_i^n$	29
	$v_{p_B}^n = \begin{cases} v_{p_{i+1}}^n, & v_{p_{i+1}}^n < 0 \\ 0, & v_{p_{i+1}}^n \geq 0 \end{cases}$	30
	$v_{p_T}^n = \begin{cases} v_{p_{i-1}}^n, & v_{p_{i-1}}^n > 0 \\ 0, & v_{p_{i+1}}^n \leq 0 \end{cases}$	31
	$F(I) = \frac{e}{\alpha\Delta z}[e^{-\gamma_2} - e^{-\gamma_1}]$	32
	$\gamma_1 = \frac{(1-\beta)I_0}{I_s} e^{-\alpha(i-1)\Delta z}$	33
	$\gamma_2 = \frac{(1-\beta)I_0}{I_s} e^{-\alpha(i)\Delta z}$	34
Growth kinetics with time decay	$v_p = \frac{2gr^2(\rho_c-\rho')A}{9\phi n}$	2
	$\mu_{net} = \mu_{g,max}F(I) - \mu_r - \mu_e - \mu_m$	25
	$\rho_{c_i}^{n+1} = \rho_{c_i}^n \mu_{net_i}^n \Delta t + \rho_{c_i}^n$	28
	$c_i^{n+1} = \frac{D_z\Delta t}{\Delta z^2}(c_{i+1}^n - 2c_i^n + c_{i-1}^n) - \frac{\Delta t}{\Delta z}\left(\lvert v_{p_i}^n c_i^n\rvert - v_{p_B}^n c_{i+1}^n - v_{p_T}^n c_{i-1}^n\right) + (\mu_{net}\Delta t + 1)c_i^n$	29
	$v_{p_B}^n = \begin{cases} v_{p_{i+1}}^n, & v_{p_{i+1}}^n < 0 \\ 0, & v_{p_{i+1}}^n \geq 0 \end{cases}$	30
	$v_{p_T}^n = \begin{cases} v_{p_{i-1}}^n, & v_{p_{i-1}}^n > 0 \\ 0, & v_{p_{i+1}}^n \leq 0 \end{cases}$	31
	$F(I) = \frac{e}{\alpha\Delta z}[e^{-\gamma_2} - e^{-\gamma_1}]$	32
	$\gamma_1 = \frac{(1-\beta)I_0}{I_s} e^{-\alpha(i-1)\Delta z}$	33
	$\gamma_2 = \frac{(1-\beta)I_0}{I_s} e^{-\alpha(i)\Delta z}$	34
	$\rho_{c_i}^{n+1} = \frac{\sum_{q=-1}^{Q}\rho_{c_i}^{n-q}W^q}{\sum_{q=-1}^{Q}W^q}$	35
	$W^q = e^{-k(t^{n+1}-t^{n-q})}$	36
Visser et al. [13]	$v_p = \frac{2gr^2(\rho_c-\rho')A}{9\phi n}$	2
	$c_i^{n+1} = \frac{D_z\Delta t}{\Delta z^2}(c_{i+1}^n - 2c_i^n + c_{i-1}^n) - \frac{\Delta t}{\Delta z}\left(\lvert v_{p_i}^n c_i^n\rvert - v_{p_B}^n c_{i+1}^n - v_{p_T}^n c_{i-1}^n\right) + (\mu_{net}\Delta t + 1)c_i^n$	29
	$v_{p_B}^n = \begin{cases} v_{p_{i+1}}^n, & v_{p_{i+1}}^n < 0 \\ 0, & v_{p_{i+1}}^n \geq 0 \end{cases}$	30
	$v_{p_T}^n = \begin{cases} v_{p_{i-1}}^n, & v_{p_{i-1}}^n > 0 \\ 0, & v_{p_{i+1}}^n \leq 0 \end{cases}$	31
	$\rho_{c_i}^{n+1} = \left(c_1 I e^{-I/I_0} + c_2\right)\Delta t + \rho_{c_i}^n$	37
	$\rho_{c_i}^{n+1} = \left(f_1\left(\rho_{c_i}^n + \rho *_{c_i}^n\right) + f_2\right)\Delta t + \rho_{c_i}^n$	38
	$I_i = \frac{I_0(1-\beta)}{-k\Delta z}(e^{-\alpha z_i} - e^{-\alpha z_{i-1}})$	39

Light function	$v_p = \frac{2gr^2(\rho_c-\rho')A}{9\phi n}$	2
	$c_i^{n+1} = \frac{D_z\Delta t}{\Delta z^2}(c_{i+1}^n - 2c_i^n + c_{i-1}^n) - \frac{\Delta t}{\Delta z}\left(\left\lvert v_{p_i}^n c_i^n\right\rvert - v_{p_B}^n c_{i+1}^n - v_{p_T}^n c_{i-1}^n\right) + (\mu_{net}\Delta t + 1)c_i^n$	29
	$v_{p_B}^n = \begin{cases} v_{p_{i+1}}^n, & v_{p_{i+1}}^n < 0 \\ 0, & v_{p_{i+1}}^n \geq 0 \end{cases}$	30
	$v_{p_T}^n = \begin{cases} v_{p_{i-1}}^n, & v_{p_{i-1}}^n > 0 \\ 0, & v_{p_{i+1}}^n \leq 0 \end{cases}$	31
	$F(I) = \frac{e}{\alpha\Delta z}[e^{-\gamma_2} - e^{-\gamma_1}]$	32
	$\gamma_1 = \frac{(1-\beta)I_0}{I_s}e^{-\alpha(i-1)\Delta z}$	33
	$\gamma_2 = \frac{(1-\beta)I_0}{I_s}e^{-\alpha(i)\Delta z}$	34
	$\rho_{c_i}^{n+1} = (c_1F(I_i^n) - c_2)\Delta t + \rho_{c_i}^n$	42
Light function with time decay	$v_p = \frac{2gr^2(\rho_c-\rho')A}{9\phi n}$	2
	$c_i^{n+1} = \frac{D_z\Delta t}{\Delta z^2}(c_{i+1}^n - 2c_i^n + c_{i-1}^n) - \frac{\Delta t}{\Delta z}\left(\left\lvert v_{p_i}^n c_i^n\right\rvert - v_{p_B}^n c_{i+1}^n - v_{p_T}^n c_{i-1}^n\right) + (\mu_{net}\Delta t + 1)c_i^n$	29
	$v_{p_B}^n = \begin{cases} v_{p_{i+1}}^n, & v_{p_{i+1}}^n < 0 \\ 0, & v_{p_{i+1}}^n \geq 0 \end{cases}$	30
	$v_{p_T}^n = \begin{cases} v_{p_{i-1}}^n, & v_{p_{i-1}}^n > 0 \\ 0, & v_{p_{i+1}}^n \leq 0 \end{cases}$	31
	$F(I) = \frac{e}{\alpha\Delta z}[e^{-\gamma_2} - e^{-\gamma_1}]$	32
	$\gamma_1 = \frac{(1-\beta)I_0}{I_s}e^{-\alpha(i-1)\Delta z}$	33
	$\gamma_2 = \frac{(1-\beta)I_0}{I_s}e^{-\alpha(i)\Delta z}$	34
	$\rho_{c_i}^{n+1} = \frac{\sum_{q=-1}^{Q}\rho_{c_i}^{n-q}W^q}{\sum_{q=-1}^{Q}W^q}$	35
	$W^q = e^{-k(t^{n+1}-t^{n-q})}$	36
	$\rho_{c_i}^{n+1} = (c_1F(I_i^n) - c_2)\Delta t + \rho_{c_i}^n$	42

Table S5. Dynamic velocity models used in particle-tracking framework.

Model	Equations	
Growth kinetics	$v_p = \frac{2gr^2(\rho_c-\rho')A}{9\phi n}$	2
	$z_{p_i}^{n+1} = z_{p_i}^n + v_{p_i}^n\Delta t + R\sqrt{6D_{z_i}^n\Delta t}$	21
	$\mu_{net} = \mu_{g,max}F(I) - \mu_r - \mu_e - \mu_m$	25
	$F(I) = \frac{I}{I_s}e^{-\frac{I}{I_s}+1}$	26
	$I(z) = (1-\beta)I_0e^{-\alpha z}$	27
	$\rho_{c_i}^{n+1} = \rho_{c_i}^n\mu_{net_i}^n\Delta t + \rho_{c_i}^n$	28
Visser et al. [13]	$v_p = \frac{2gr^2(\rho_c-\rho')A}{9\phi n}$	2
	$z_{p_i}^{n+1} = z_{p_i}^n + v_{p_i}^n\Delta t + R\sqrt{6D_{z_i}^n\Delta t}$	21
	$I(z) = (1-\beta)I_0e^{-\alpha z}$	27
	$\rho_{c_i}^{n+1} = \left(c_1Ie^{-I/I_0} + c_2\right)\Delta t + \rho_{c_i}^n$	37
	$\rho_{c_i}^{n+1} = \left(f_1\left(\rho_{c_i}^n + \rho_*\right) + f_2\right)\Delta t + \rho_{c_i}^n$	38

Light function	$v_p = \frac{2gr^2(\rho_c - \rho')A}{9\phi n}$	2
	$z_{p_i}^{n+1} = z_{p_i}^n + v_{p_i}^n \Delta t + R\sqrt{6D_{z_i}^n \Delta t}$	21
	$F(I) = \frac{I}{I_s} e^{-\frac{I}{I_s}+1}$	26
	$\rho_{c_i}^{n+1} = (c_1 F(I_i^n) - c_2)\Delta t + \rho_{c_i}^n$	42

2. Model Result Plots

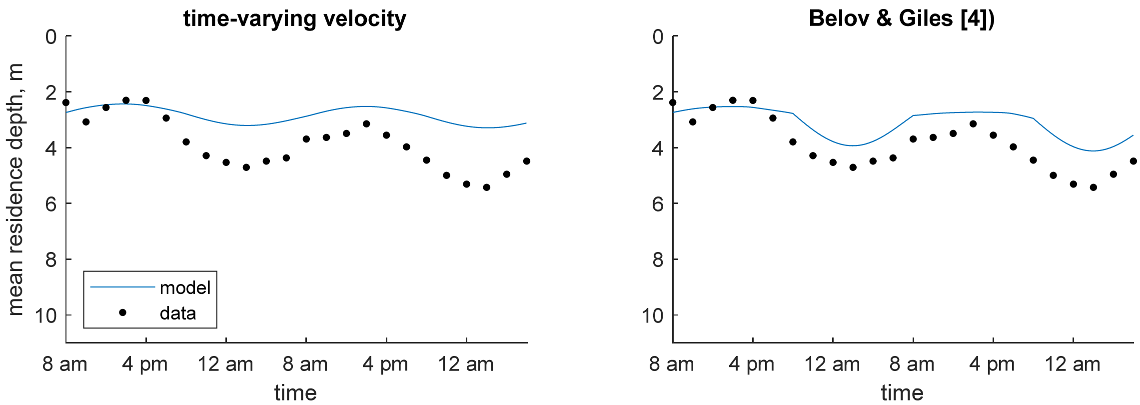

Figure S1. Time series of observed and predicted mean residence depth of chlorophyll a concentration in Shennong Stream enclosure site using predefined velocity models (continuum).

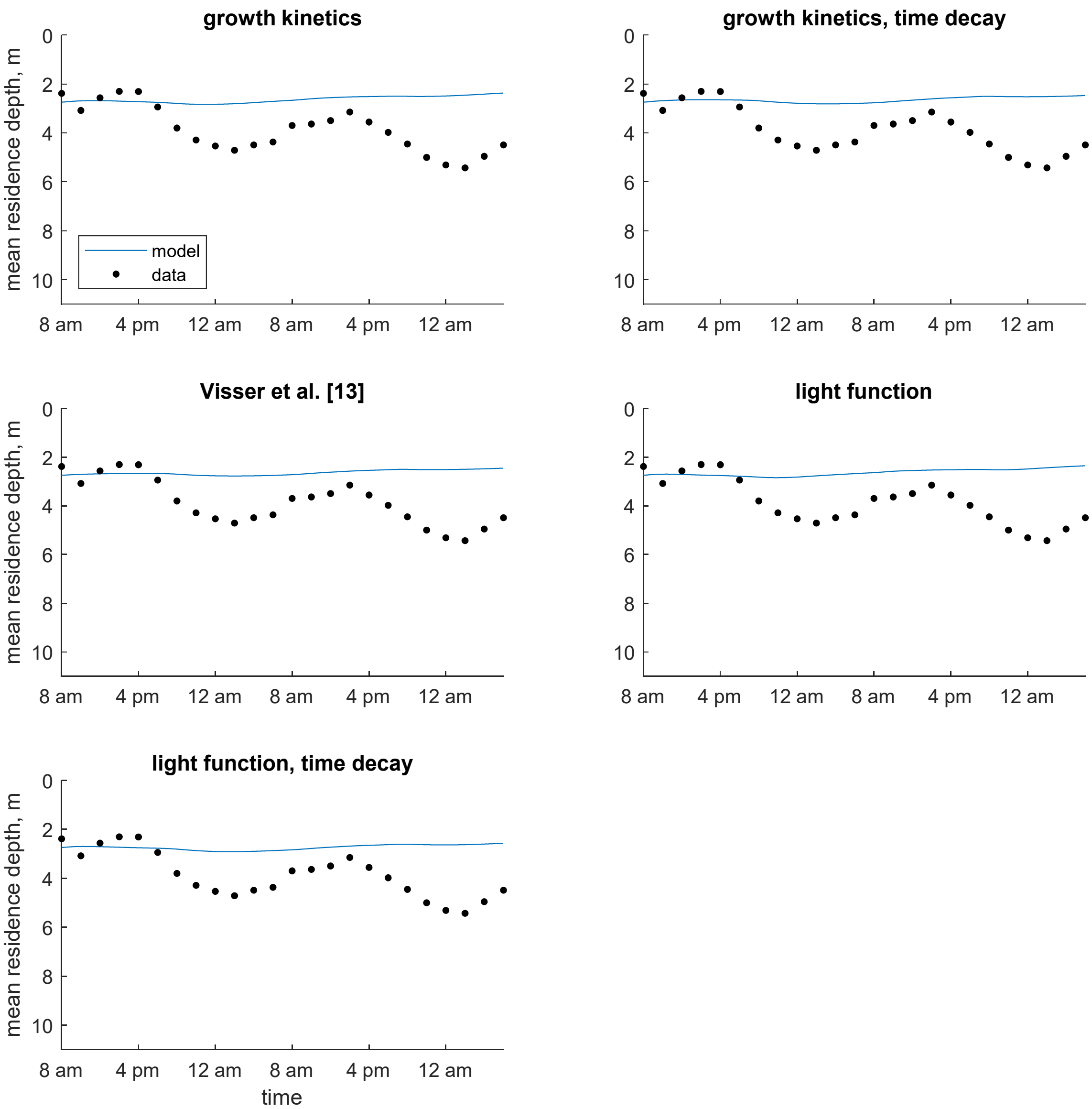

Figure S2. Time series of observed and predicted mean residence depth of chlorophyll a concentration in Shennong Stream enclosure site using dynamic velocity models (continuum).

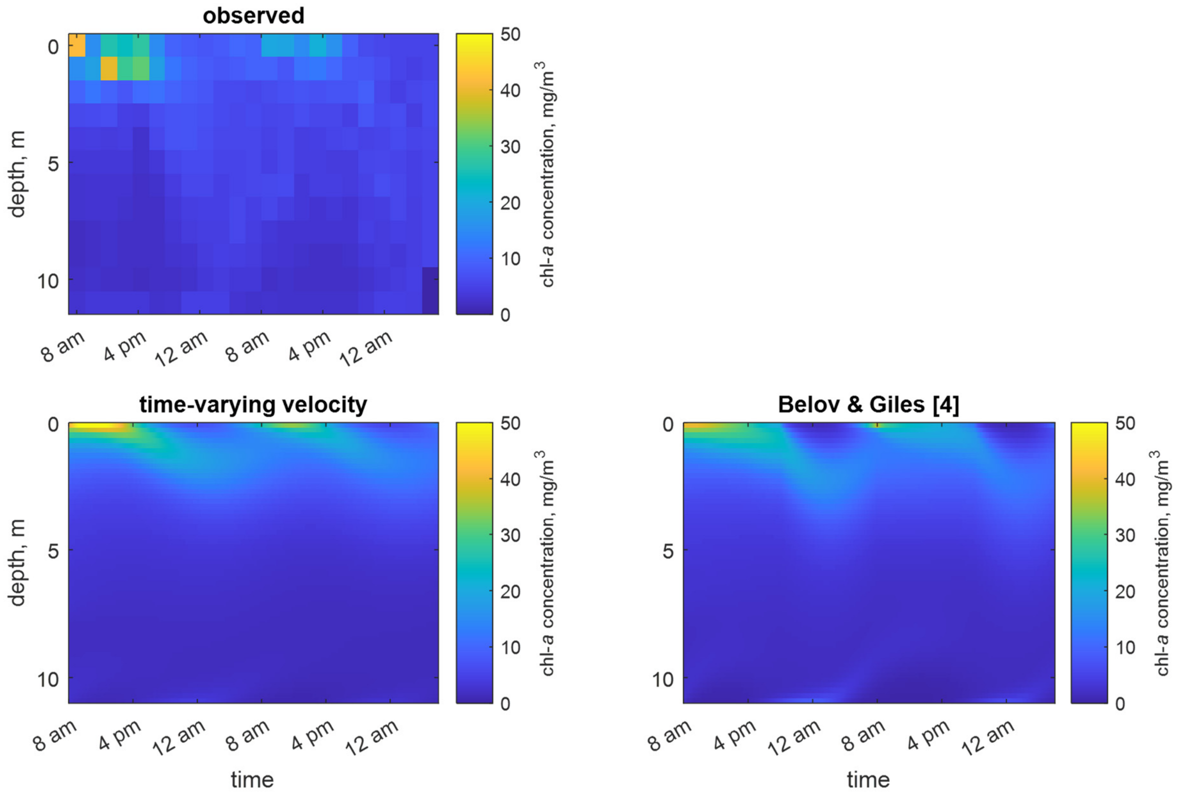

Figure S3. Time series of observed and predicted chlorophyll a concentration in Shennong Stream enclosure site using predefined velocity models (continuum).

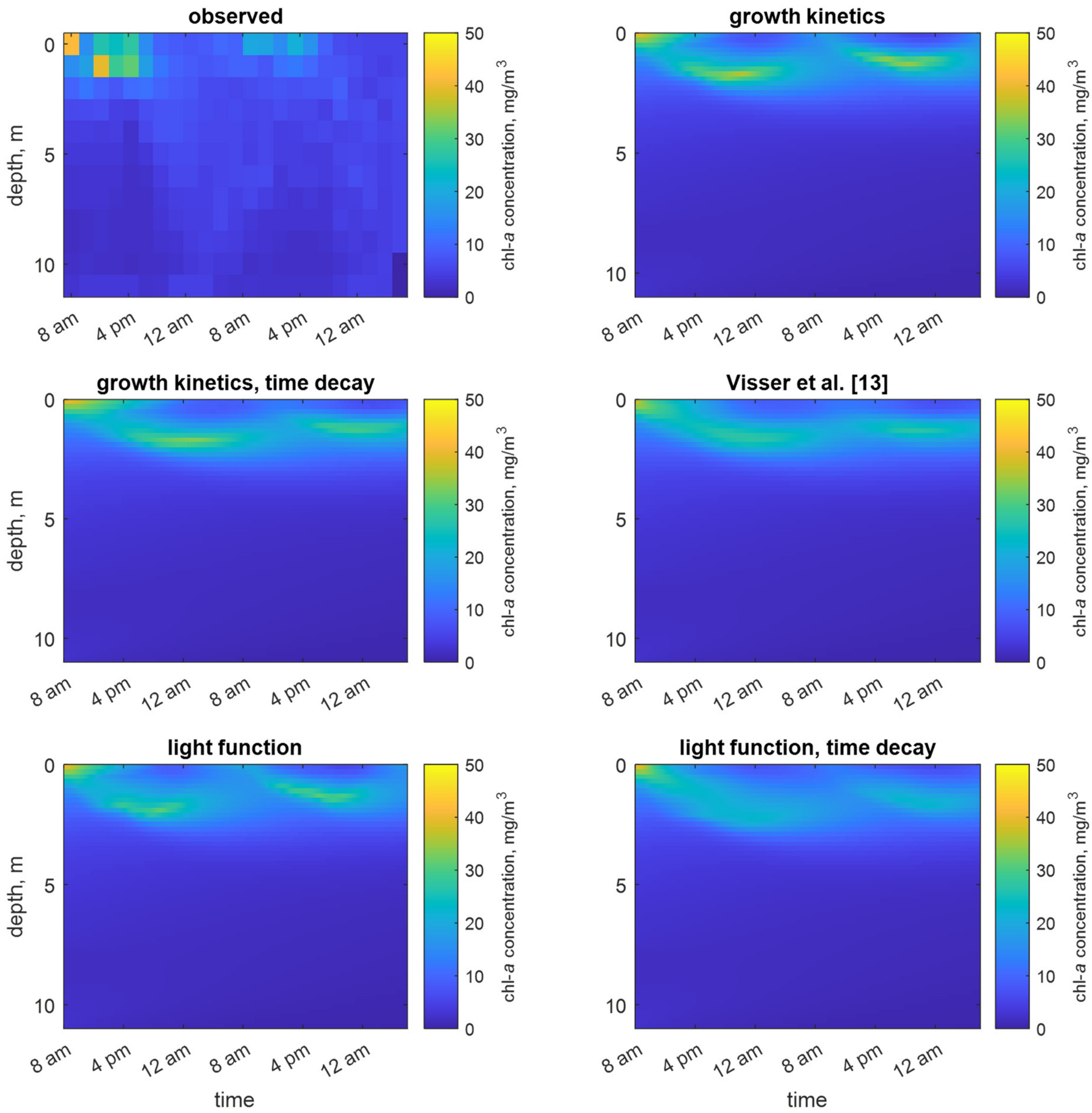

Figure S4. Time series of observed and predicted chlorophyll a concentration in Shennong Stream enclosure site using dynamic velocity models (continuum).

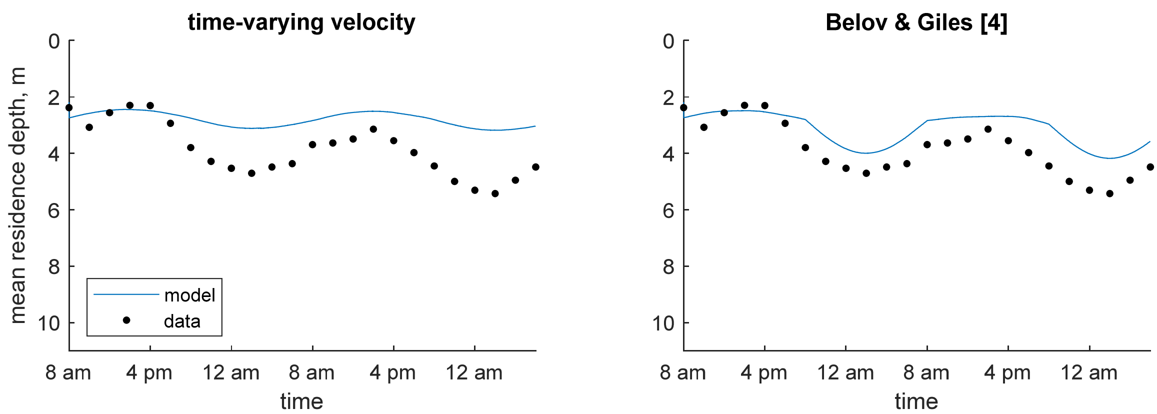

Figure S5. Time series of observed and predicted mean residence depth of chlorophyll a concentration in Shennong Stream enclosure site using predefined velocity models (particle-tracking).

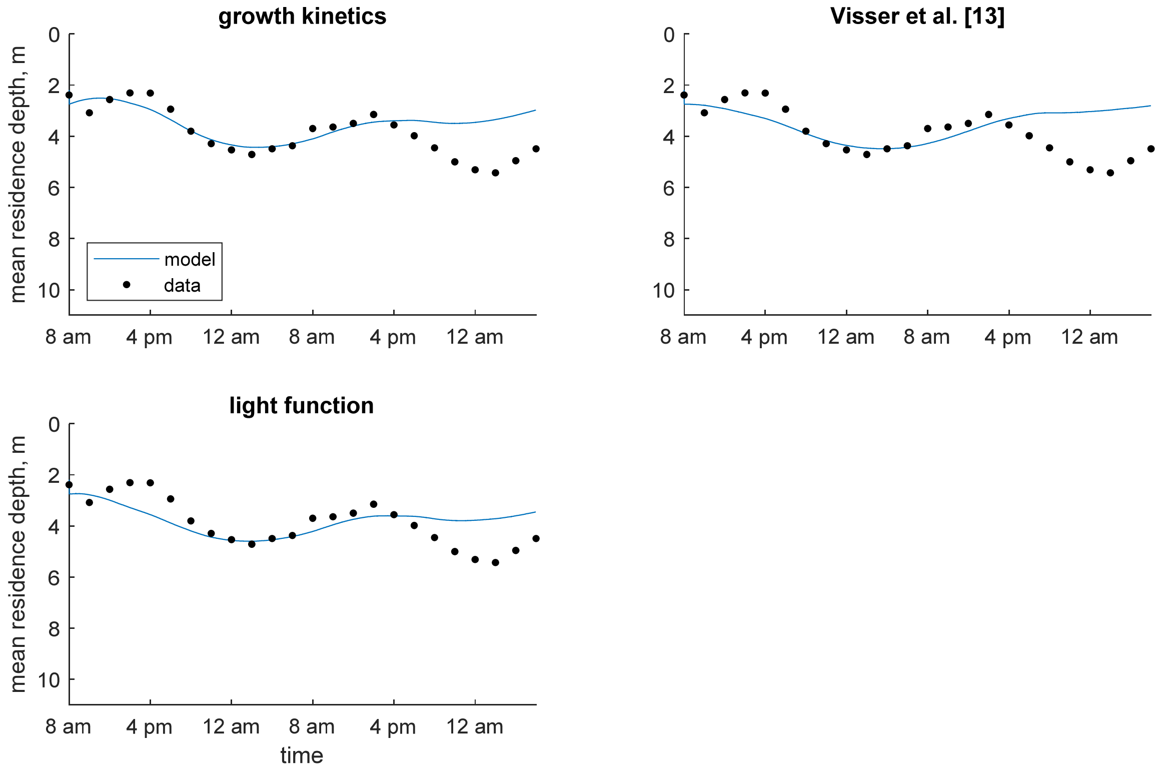

Figure S6. Time series of observed and predicted mean residence depth of chlorophyll a concentration in Shennong Stream enclosure site using dynamic velocity models (particle-tracking).

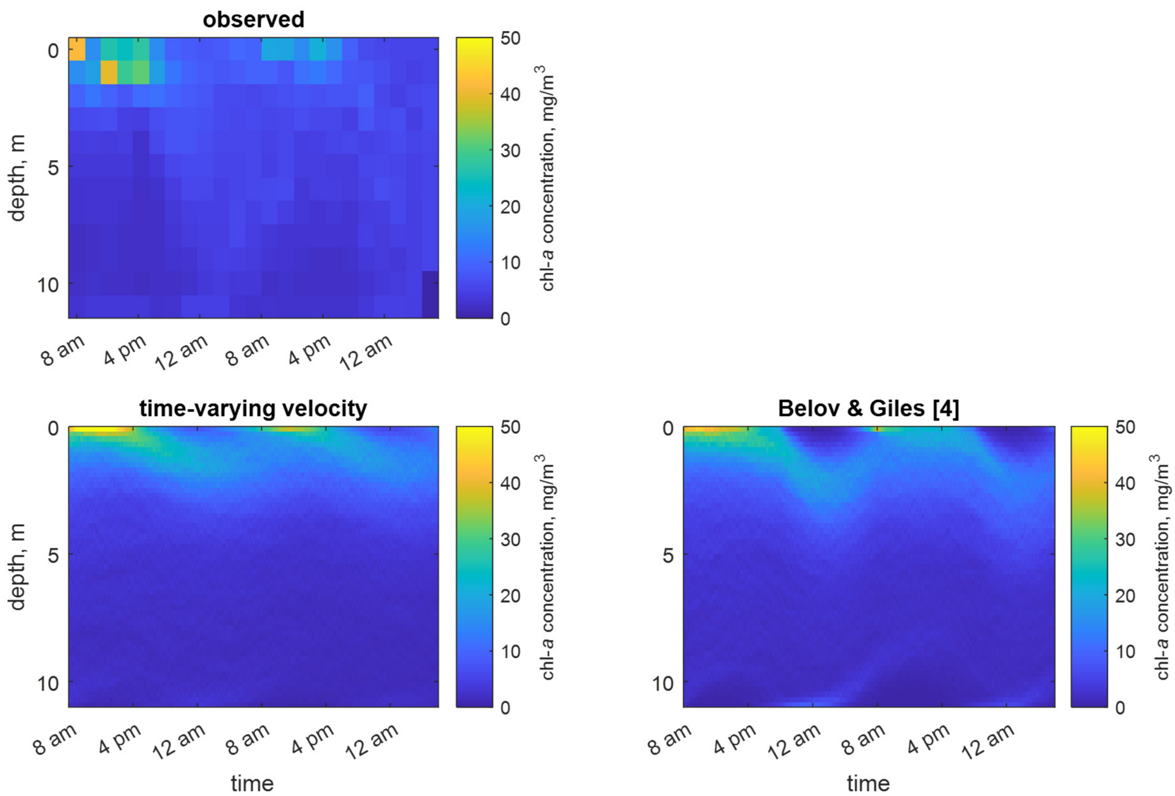

Figure S7. Time series of observed and predicted chlorophyll a concentration in Shennong Stream enclosure site using predefined velocity models (particle-tracking).

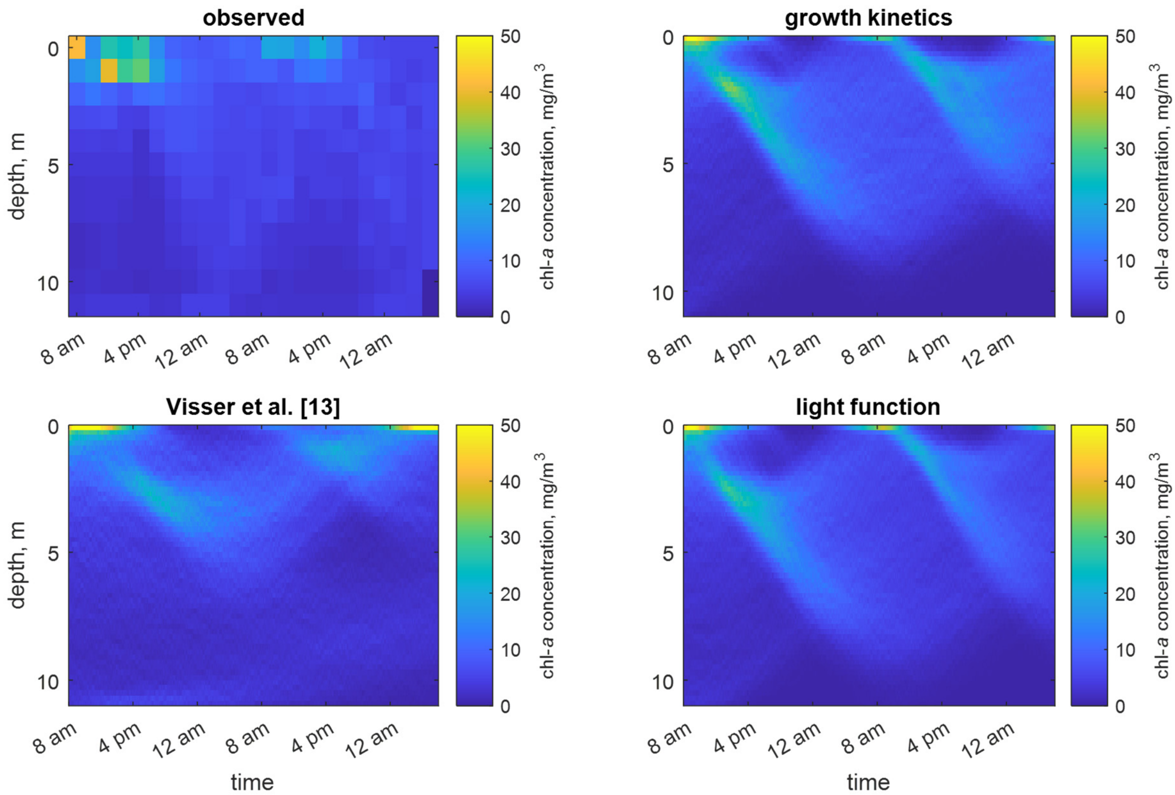

Figure S8. Time series of observed and predicted chlorophyll a concentration in Shennong Stream enclosure site using dynamic velocity models (particle-tracking).

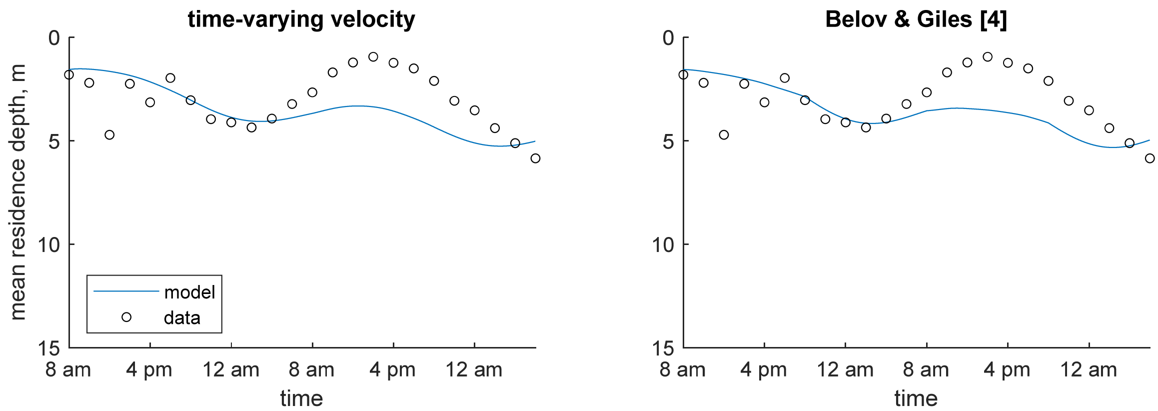

Figure S9. Time series of observed and predicted mean residence depth of chlorophyll a concentration in Shennong Stream open water site using predefined velocity models (continuum).

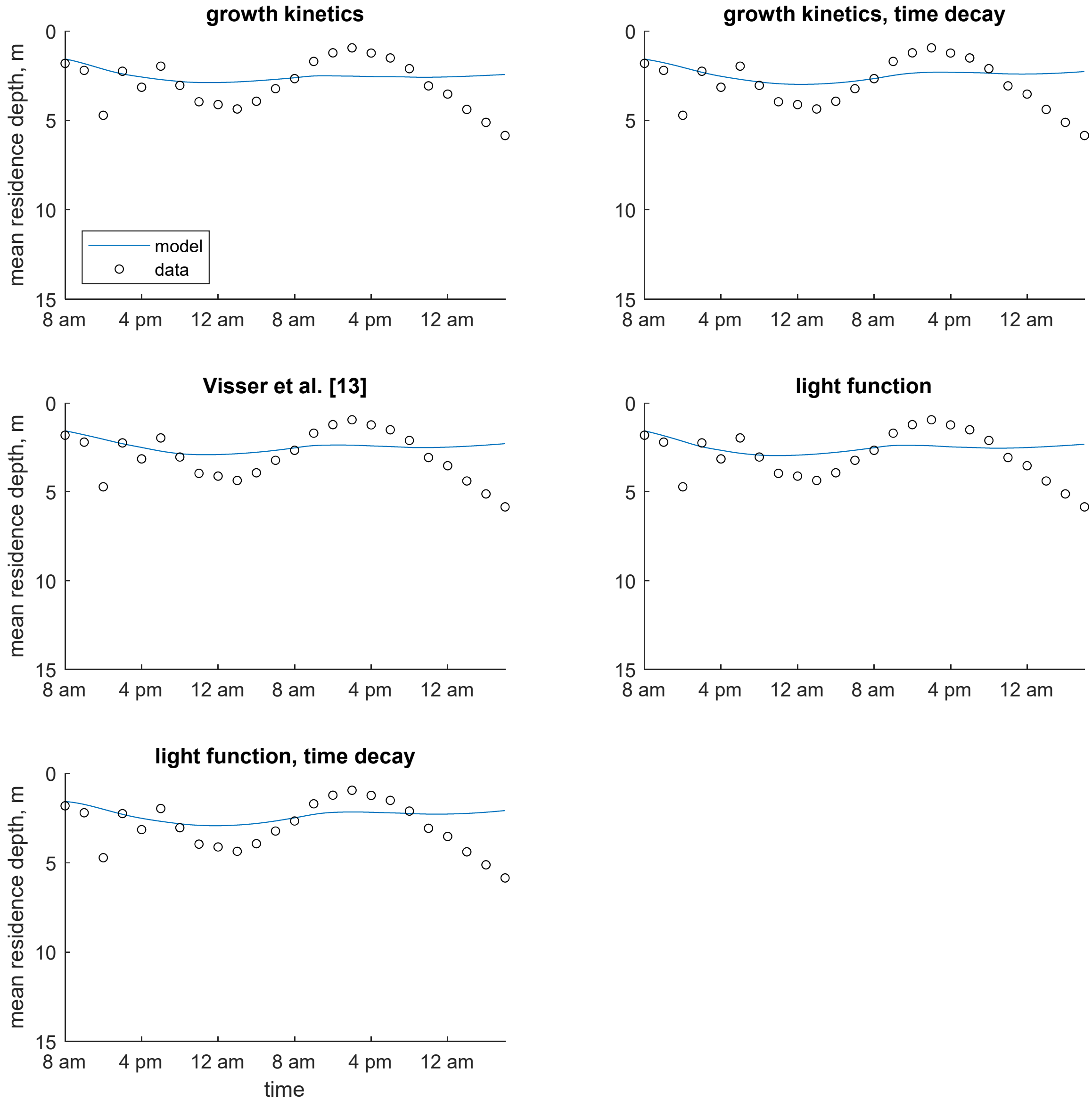

Figure S10. Time series of observed and predicted mean residence depth of chlorophyll a concentration in Shennong Stream open water site using dynamic velocity models (continuum).

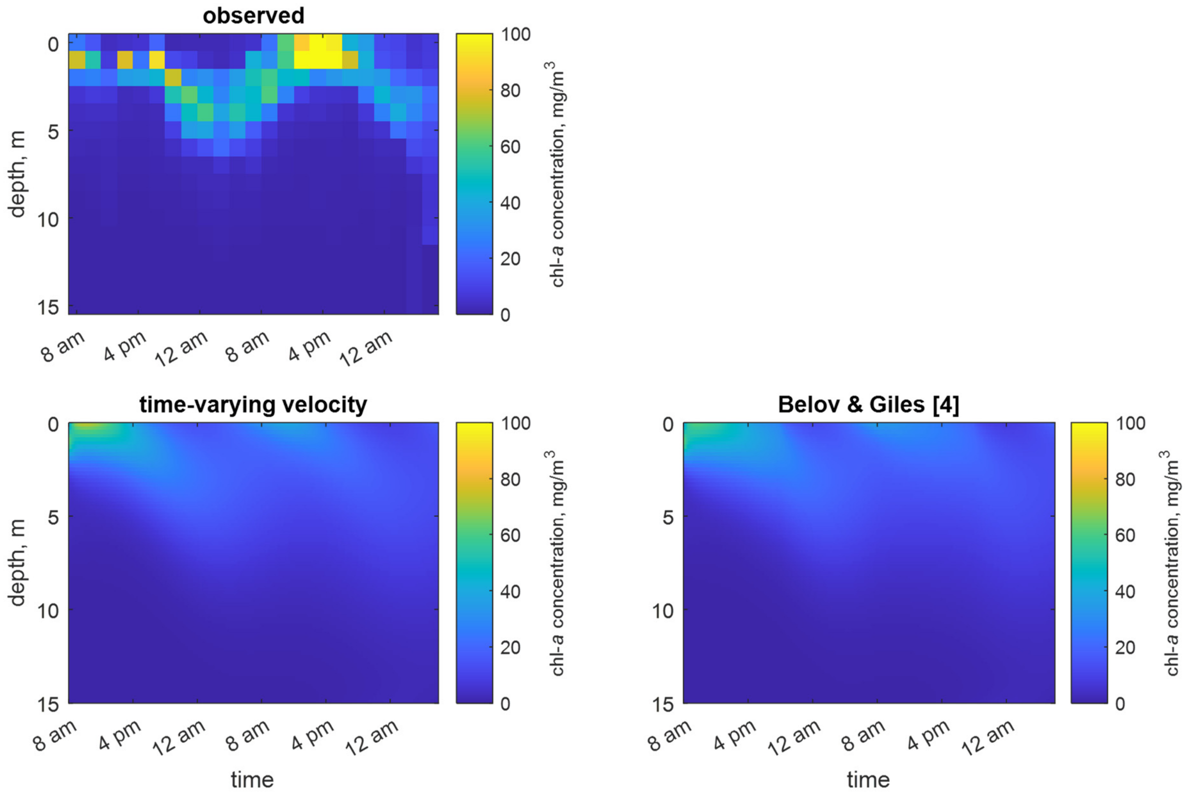

Figure S11. Time series of observed and predicted chlorophyll a concentration in Shennong Stream open water site using predefined velocity models (continuum).

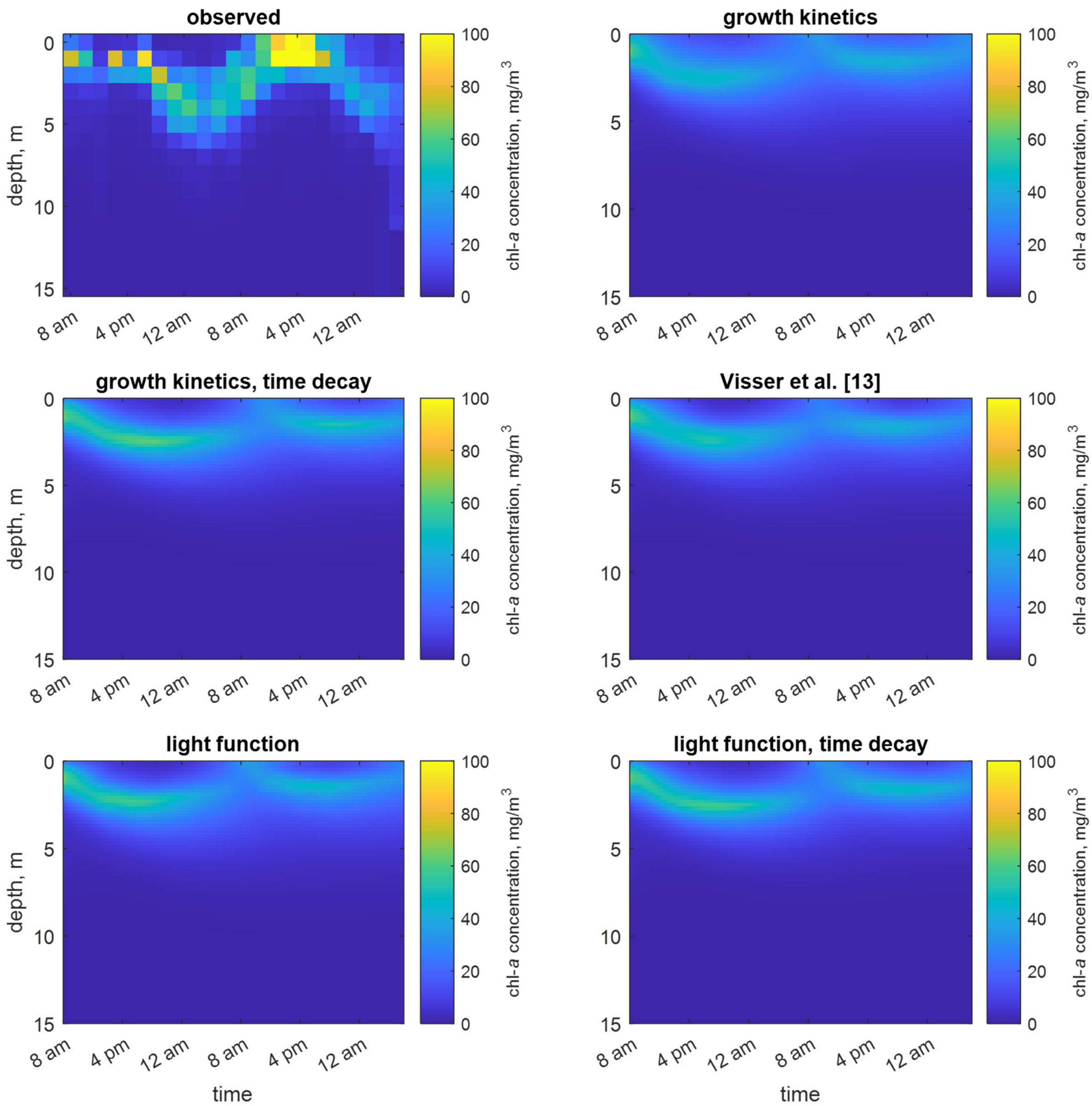

Figure S12. Time series of observed and predicted chlorophyll a concentration in Shennong Stream open water site using dynamic velocity models (continuum).

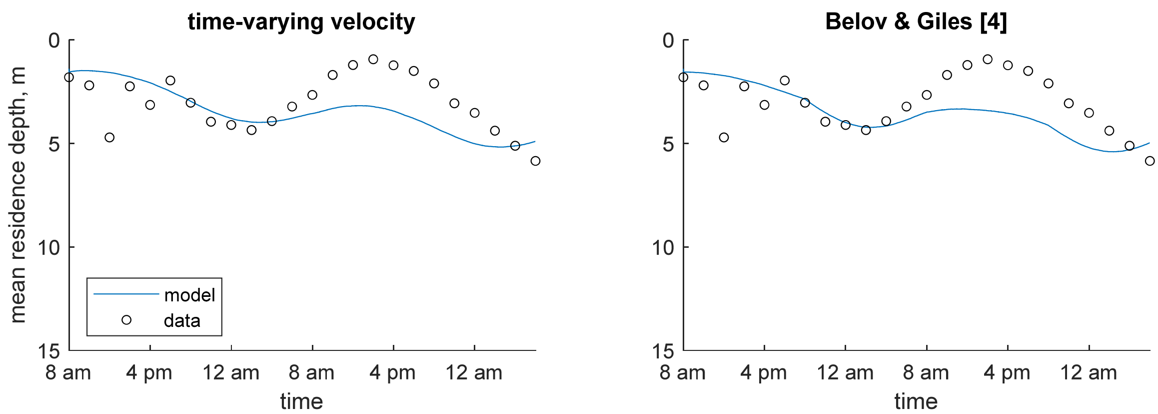

Figure S13. Time series of observed and predicted mean residence depth of chlorophyll a concentration in Shennong Stream open water site using predefined velocity models (particle-tracking).

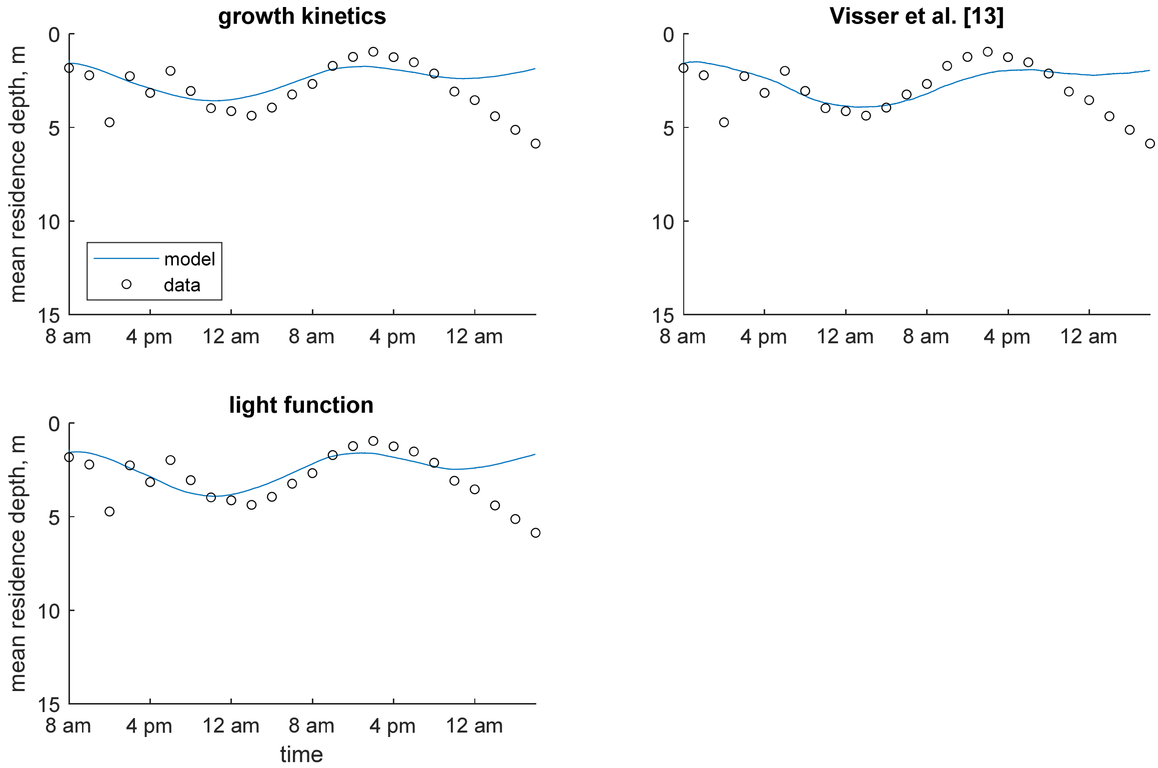

Figure S14. Time series of observed and predicted mean residence depth of chlorophyll a concentration in Shennong Stream open water site using dynamic velocity models (particle-tracking).

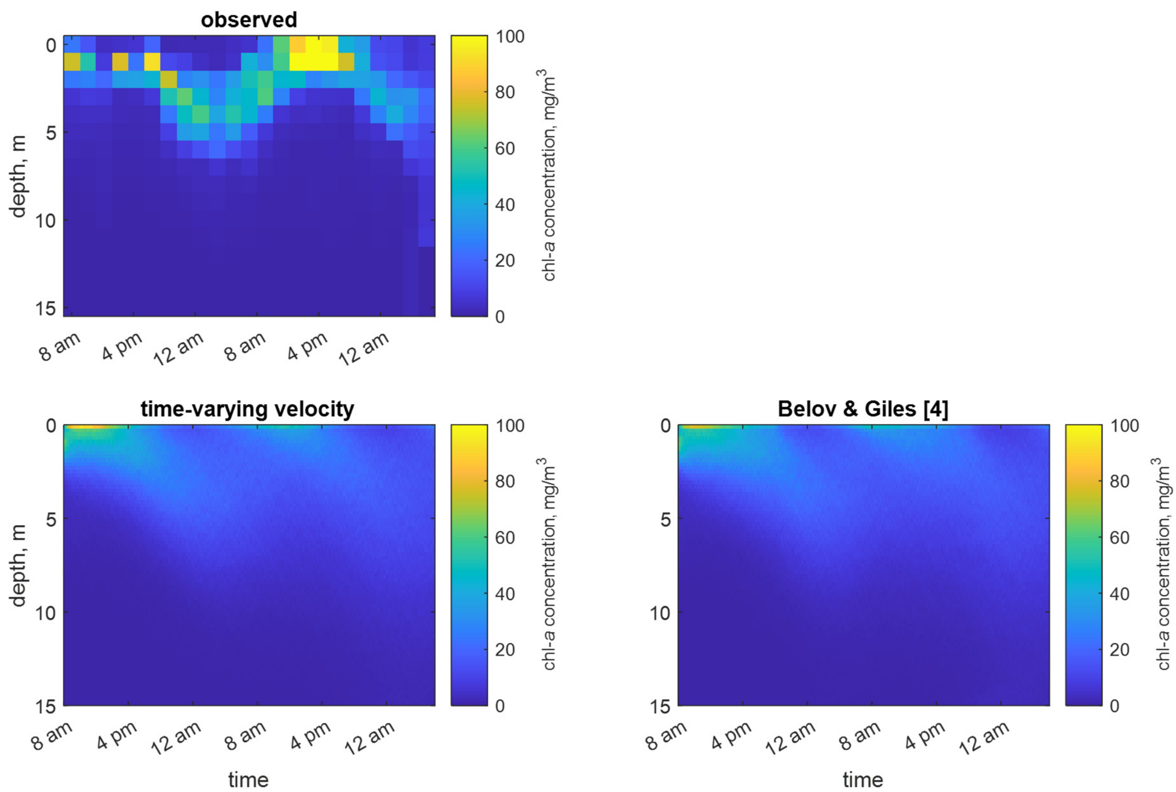

Figure S15. Time series of observed and predicted chlorophyll a concentration in Shennong Stream open water site using predefined velocity models (particle-tracking).

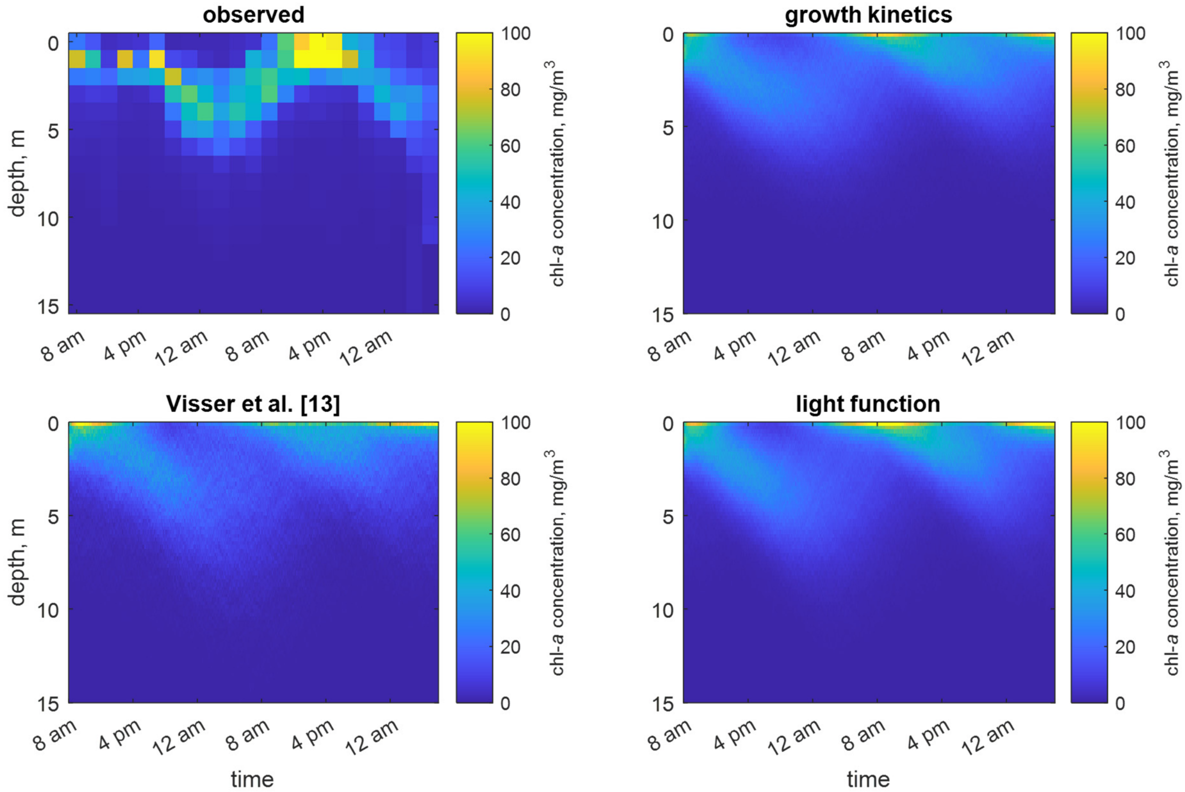

Figure S16. Time series of observed and predicted chlorophyll a concentration in Shennong Stream open water site using dynamic velocity models (particle-tracking).

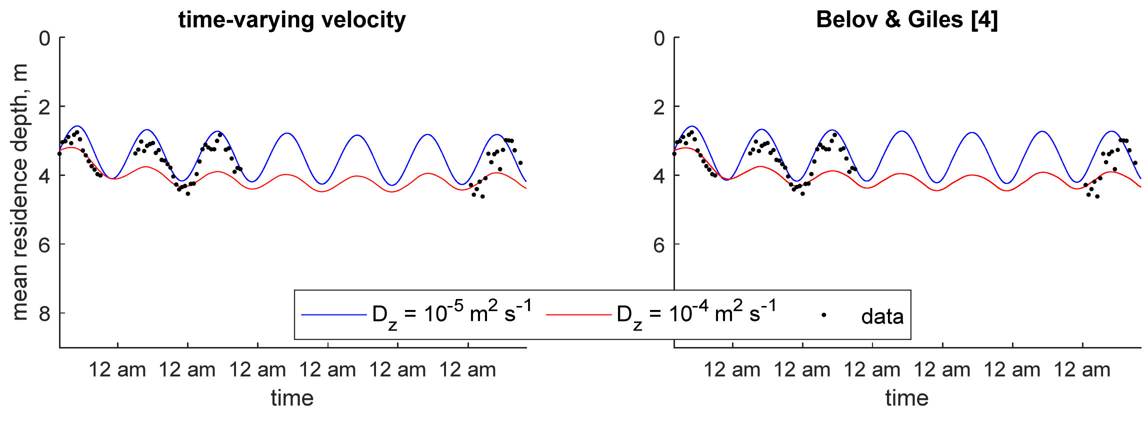

Figure S17. Time series of observed and predicted mean residence depth of chlorophyll a concentration in Xiangxi Bay using predefined velocity models (continuum).

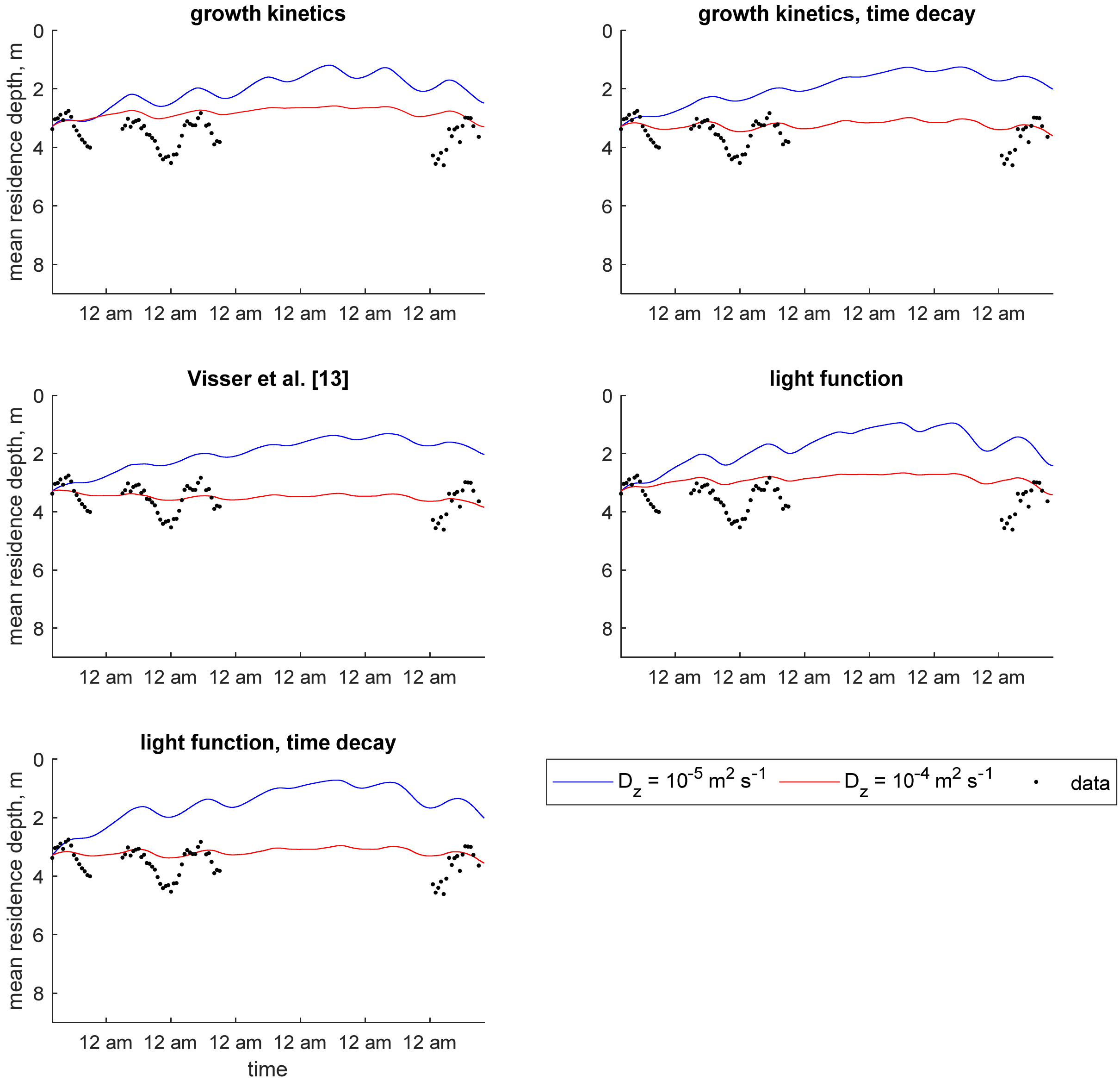

Figure S18. Time series of observed and predicted mean residence depth of chlorophyll a concentration in Xiangxi Bay using dynamic velocity models (continuum).

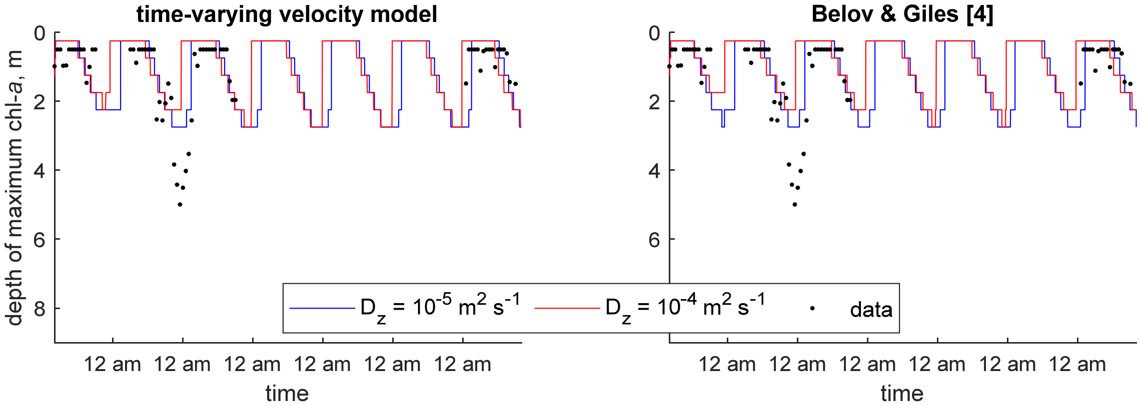

Figure S19. Time series of observed and predicted depth of maximum chlorophyll a concentration in Xiangxi Bay using predefined velocity models (continuum).

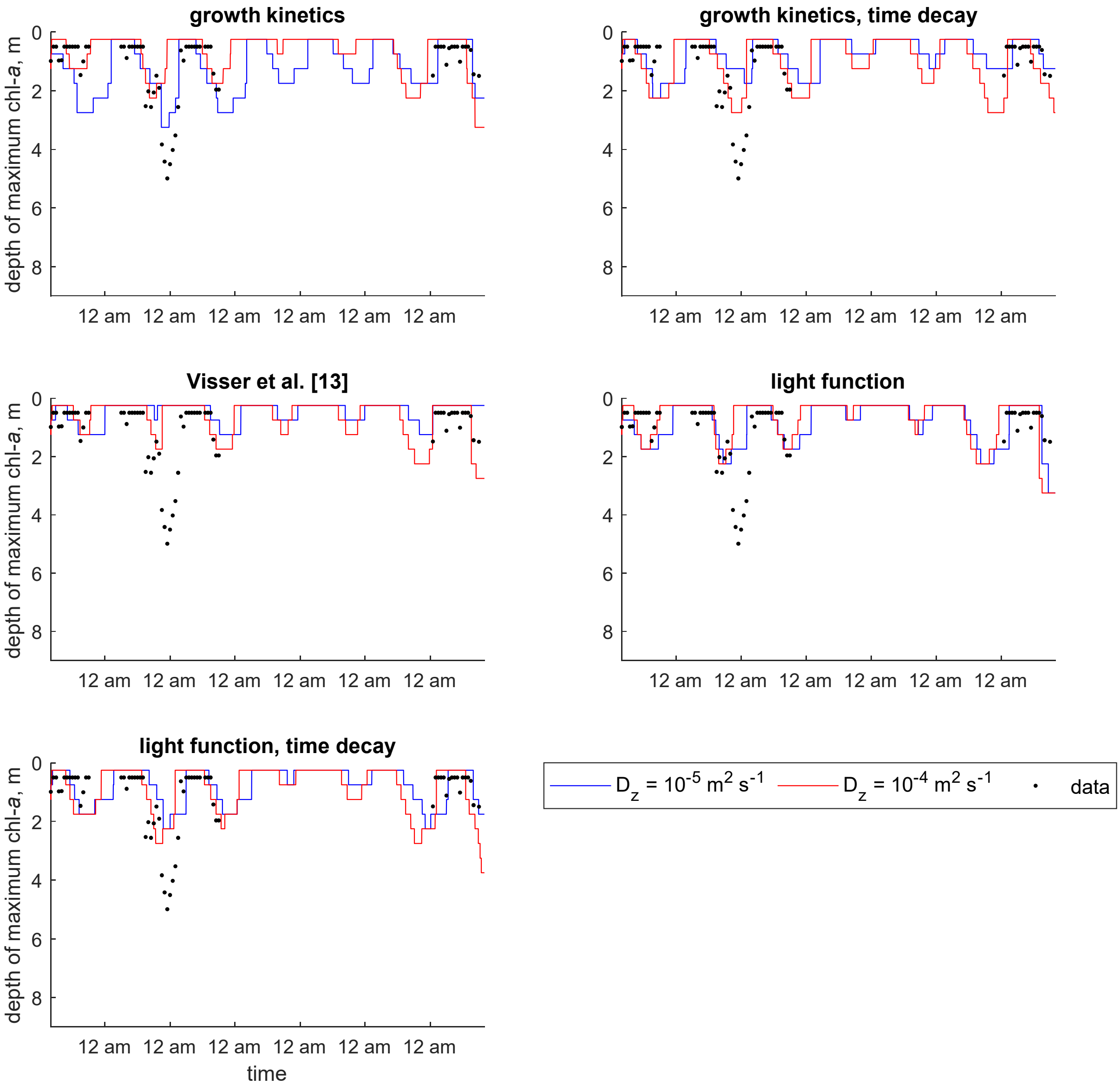

Figure S20. Time series of observed and predicted depth of maximum chlorophyll a concentration in Xiangxi Bay using dynamic velocity models (continuum).

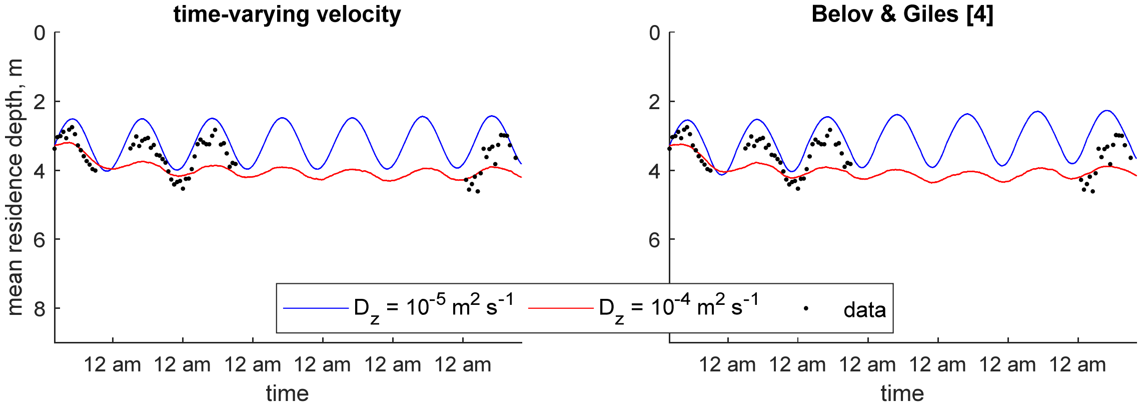

Figure S21. Time series of observed and predicted mean residence depth of chlorophyll a concentration in Xiangxi Bay using predefined velocity models (particle-tracking).

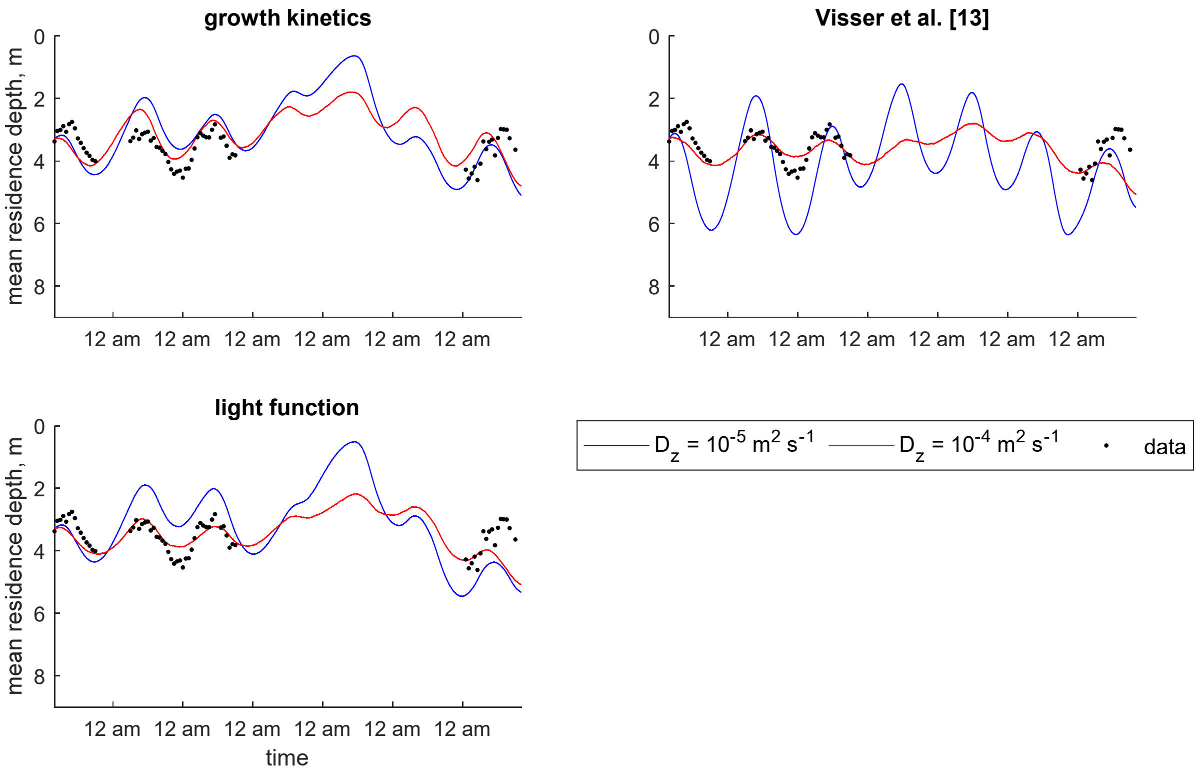

Figure S22. Time series of observed and predicted mean residence depth of chlorophyll a concentration in Xiangxi Bay using dynamic velocity models (particle-tracking).

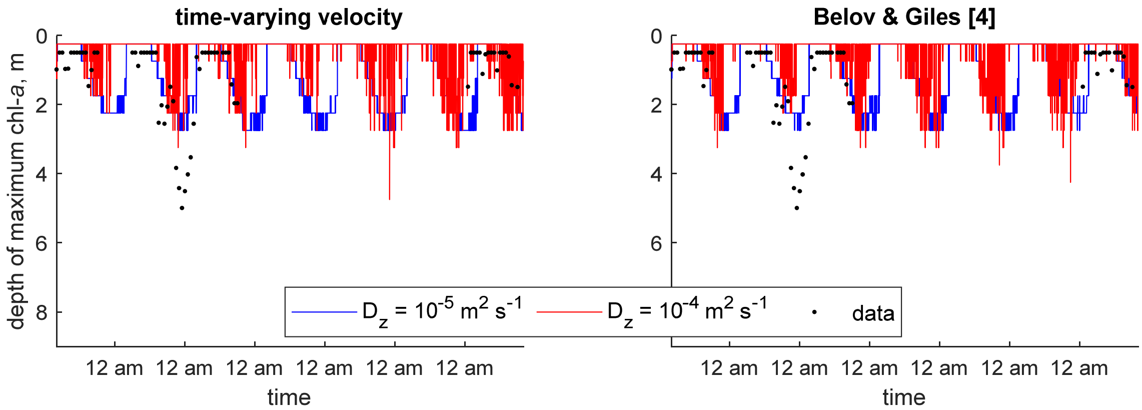

Figure S23. Time series of observed and predicted depth of maximum chlorophyll a concentration in Xiangxi Bay using predefined velocity models (particle-tracking).

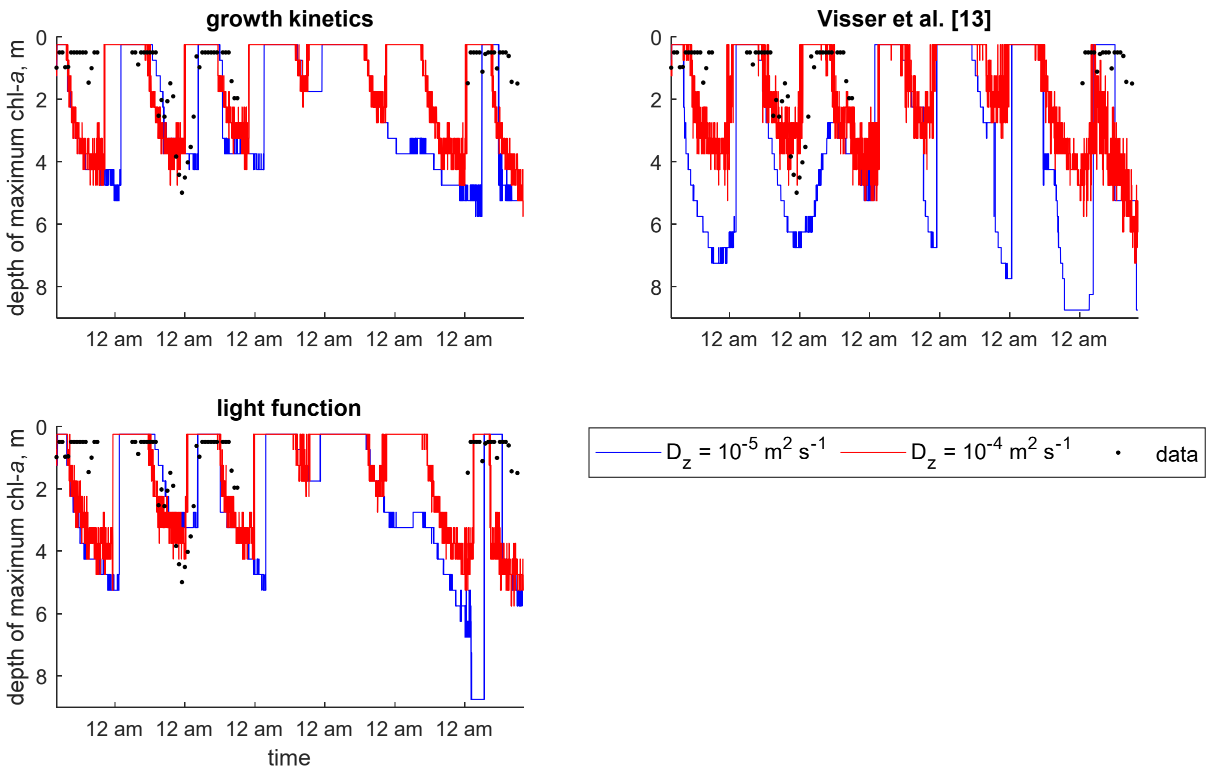

Figure S24. Time series of observed and predicted depth of maximum chlorophyll a concentration in Xiangxi Bay using dynamic velocity models (particle-tracking).